Paper published in:

B. Balzano, A.W. Bruno, H. Denzer, D. Molan, A. Tarantino and D. Gallipoli (2021).

REAL-TIME quality check of measurements of soil water status in the vadose zone.

Physics and Chemistry of the Earth, 121: 102918

https://doi.org/10.1016/j.pce.2020.102918

REAL-TIME QUALITY CHECK OF MEASUREMENTS OF SOIL WATER STATUS IN THE VADOSE ZONE

Brunella Balzano[1], Agostino Walter Bruno[2], Heiner Denzer[3], Denis Molan[3], Alessandro Tarantino[4], Domenico Gallipoli[5]

[1] Cardiff University, School of Engineering, Queen's Building, Cardiff

[2] School of Engineering, Geotechnics and Structures GEST, Newcastle University, Newcastle, United Kingdom

[3] PESSL Instruments, Weiz, Austria

[4] University of Strathclyde, Department of Civil and Environmental Engineering, Glasgow, United Kingdom

[5] Dipartimento di Ingegneria Civile, Chimica e Ambientale, Università degli Studi di Genova, Genoa, Italy.

CORRESPONDING AUTHOR: -
Dr Brunella Balzano
School of Engineering
Cardiff University
Queen's Building, The Parade
CF243AA

Email: balzanob@cardiff.ac.uk

ABSTRACT

The in-situ monitoring of soil suction and water content is important for a range of applications from civil engineering (e.g. estimation of groundwater infiltration) to agriculture (e.g. optimization of irrigation). The efficiency of field monitoring systems has recently improved thanks to the development of sensors that continuously record soil water status data and remotely transmit them through the internet. These data are, however, accessed by users only on a periodic basis, which impedes a timely detection of sensor failures. To overcome this limitation, this paper describes a method for automatically assessing the quality of suction and water content measurements in the field. The method is based on a real time comparison between field data and a reference a soil-water retention curve. A tolerance box is introduced around each field data point, defined by a pair of suction and water content measurements. If the tolerance box intersects the reference soil-water retention curve, the suction and water content sensors are assumed to work correctly. Conversely, if the tolerance box falls outside the reference soil-water retention curve outside, at least one of the two sensors may have failed. The proposed method has been validated against measurements from five different agricultural soils confirming the efficiency of the tool in evaluating the accuracy of field data.

KEYWORDS

Suction – water content – soil-water retention curve – monitoring system – data quality control – soil-atmosphere interaction.

1 INTRODUCTION

Soil in the vadose zone is a natural resource that provides nutrients to vegetation, hosts important biological activities and acts as an interface for air-water interaction. The sustainable exploitation of the ground and the preservation of the land's health are matters of utmost concern for engineers, geologists, farmers, soil scientists and land managers (Stenberg, 1999). In this context, field monitoring of geohydrological variables may be a very useful tool for a range of applications, provided that suitable strategies are put in place for assessing the reliability of recorded data (Mendes et al., 2008; Supit et al., 2012; Molchanov, 2013; Pooja et al., 2017).

The farming industry makes use of field stations to monitor climatic variables (e.g. intensity of rainfall, wind, solar radiation, relative humidity and air temperature) as well as soil water status variables (e.g. pore-water pressure and water content). In many cases, the recorded data are transmitted to remote servers in real time, via wireless data connections, but are only consulted by users on a periodic basis (Vicente-Guijalba et al., 2014). Therefore, in the absence of an automated warning system, any malfunctioning of the sensors may be overlooked and discovered only at the next user access. Crucial soil information may then be lost or misinterpreted with potentially serious consequences for the relevant application. To address this limitation, the present work develops an automated method for assessing the reliability of in-situ measurements of suction (i.e. the difference between pore air and water pressures) and volumetric water content (i.e. the ratio of the water volume to the total soil volume). This data assessment method relies on a consistency check between the field measurements and a reference water retention curve.

A variety of soil-water retention models have been proposed ranging from simple unique relationships between water content and suction (Brooks and Corey, 1964; Van Genuchten, 1980; Fredlund and Xing, 1994) to more complex laws where the retention behaviour depends also on soil deformation

(Gallipoli et al., 2003; Sun et al., 2008; Mašín, 2010; Salager et al., 2010) and/or hydraulic hysteresis (Wheeler et al., 2003; Khalili et al., 2008; Nuth and Laloui, 2008; Tarantino, 2009; Gallipoli, 2012; Zhou et al., 2012; Gallipoli et al., 2015). The present work employs the well-established pedotransfer function of Vereecken et al. (1989), built upon a van Genuchten- type function (van Genucthen, 1980) to define the reference water retention function.

Water retention model parameters are generally calibrated by means of laboratory tests, which are time consuming and costly, making the characterization of large areas virtually impossible. In this respect, pedotransfer functions offer an appealing alternative via the use of empirical correlations between retention model parameters and easily measurable physical soil properties. For example, the pedotransfer function of Vereecken et al. (1989) relates the parameters of van Genuchten-type function to intrinsic soil properties such as grain size distribution, dry density and carbon content. Pedotransfer functions neglect, however, the dependency of the retention behaviour on the structure of the soil, which is the consequence of material history including past exposure to mechanical, wetting and drying actions (Weynants et al., 2009).

The reference water retention function was first calibrated based on soil measurements from five different agricultural sites in Austria, France and Italy, where field stations had been installed. The reference water retention function was then assessed against additional field measurements not used during calibration and by means of Finite Element simulations of groundwater infiltration at the monitored sites.

The data quality assessment criterion consists in the definition of a tolerance box around each field data point identified by a pair of simultaneous suction and water content measurements. If this tolerance box intersects the reference soil-water retention curve, the sensors are assumed to work correctly whereas at least one of the sensors is assumed to have failed if tolerance box does not intersect the reference water retention curve. The size of the tolerance box is defined considering the

uncertainties of the retention model and the potential inaccuracies of field measurements. This criterion has been successfully applied to measurements from a field station in Austria, demonstrating the ability of the approach to detect potential sensor failures with no human intervention.

Finally, it is worth mentioning that the proposed method has been here employed to monitor measurements in agricultural land but it can be extended to civil engineering applications (e.g. monitoring of soil slopes), possibly by using more accurate models for the soil-water retention function.

2 REFERENCE SOIL-WATER RETENTION CURVE

$$\theta = \theta_r + (\theta_s - \theta_r)\,\frac{1}{1 + \left(\alpha \frac{s}{\gamma_w}\right)^n} \tag{1}$$

where $\boldsymbol{\theta}$ is the volumetric water content, $\boldsymbol{s}$ is the suction, and θ_r, θ_s, α and n are model parameters (θ_r and θ_s are the residual and saturated volumetric water contents respectively and γ_w is the specific weight of the water that is typically assumed to be 10 kN/m^3). After analysing forty different soils from sands to heavy clays, Vereecken et al. (1989) proposed the following relationships between the above model parameters and the particle grading, carbon content and dry density of the soil:

$$\theta_r = 0.015 + 0.005\ \%Clay + 0.014\ \%C \tag{2}$$

$$\theta_s = 0.81 - 0.283\ \rho_d + 0.001\ \%Clay \tag{3}$$

$$\alpha = e^{\left(-2.486 + 0.025\ \%Sand - 0.351\ \%C - 2.617\rho_d - 0.023\ \%Clay\right)} \quad [1/cm] \tag{4}$$

$$n = e^{\left(0.053 - 0.009\ \%Sand - 0.013\ \%Clay + 0.00015\ \%Sand^2\right)} \tag{5}$$

where $\%Clay$ and $\%Sand$ are the clay and sand fractions, respectively, $\%C$ is the carbon content and ρ_d is the dry density of the soil in g/cm^3. All four water retention model parameters θ_r, θ_s, α and n can therefore be defined on the basis of four easily measurable soil properties. This is particularly

advantageous because it allows the estimation of the water retention curve for those cases where direct calibration of water retention parameters through laboratory tests is expensive or time consuming, as is often the case in agricultural applications.

Even if data about particle grading, carbon content, and dry density are not available and water retention model parameters need to be estimated by fitting field data (as shown later in the paper), it is convenient to best-fit physical properties (%Clay, %Sand, %C, ρ_d) rather than the parameters θ_s, θ_r, α, and n, because 'best-fitting' physical properties can be more easily verified by visual inspection of soil samples in the field.

The choice of a relatively simple soil-water retention model, which does not incorporate the effects of soil deformations and hydraulic hysteresis, has here been made to facilitate application of the proposed data assessment method to real cases. Moreover, the absence of soil deformation monitoring would render the use of more sophisticated retention models unfeasible at this stage. Clearly, the disregard of both soil deformation and hydraulic hysteresis generates a deviation of the predictions of the soil-water retention curve from field data but this deviation is here accounted for by defining a relatively large tolerance box around each data point. This is acceptable for agricultural purposes but may be less acceptable for civil engineering applications (e.g. monitoring of soil slopes). In this case, further refinements are possible to incorporate additional aspects of soil behaviour and, hence, to increase the accuracy of the water retention model.

3 SUCTION AND VOLUMETRIC WATER CONTENT DATA

Field stations are relatively common in agriculture to monitor climatic variables affecting crops growth such as rainfall, wind, solar radiation, relative humidity and temperature. Weather monitoring is often performed by multiple sensors connected to a single recording unit that broadcasts data remotely through the internet (Figures 1a and 1b). Field stations may also be equipped with additional

sensors to measure soil water status variables such as suction and water content. These additional measurements provide important information about the state of the soil and can help optimising irrigation to achieve maximum crop yield with minimum water consumption.

This paper proposes a method to assess automatically the reliability of suction and volumetric water content measurements with the objective of detecting potential sensor failures. The method has been applied to field measurements collected from five stations installed by the company Pessl Instruments (Weiz, Austria) in five different agricultural sites in Austria, France and Italy. Each of these stations is equipped with standard sensors to record weather variables as well as additional sensors to monitor soil suction and volumetric water content. Table 1 indicates the identification code of each station together with the site where the station was installed and the relevant soil sensors. The characteristics of the suction and volumetric water content sensors connected to the different stations are briefly described in the following sections.

3.1 Measurement of suction

Three different sensors were used to measure soil suction, namely the MPS-1 sensor, the MPS-6 sensor and the Universal Tensiometer. The MPS-1, which is commercialised by the company Meter Environment (Pullman, USA), measures suctions between 10 kPa and 500 kPa with an accuracy of ±5 kPa and a resolution of 1 kPa over the range from 10 to 50 kPa. For values of suction larger than 50 kPa, the accuracy becomes ±20% of the reading value and the resolution increases to 4 kPa. The MPS-6 sensor, which is also commercialised by the company Meter Environment (Pullman, USA), measures suctions between 10 kPa and 100 kPa with an accuracy of ±10% of the reading value and a resolution of 0.1 kPa. The Universal Tensiometer, which has been developed at the Université de Pau et des Pays de l'Adour in France (Mendes et al., 2016; Mendes et al., 2018) can instead measure suctions over a much wider range, i.e. between 0 kPa and 1500 kPa, with an accuracy of about ±10 kPa and a resolution of 1 kPa.

3.2 Measurement of volumetric water content

Two different sensors were used to measure the volumetric water content of the soil, namely the 10HS sensor and the EC-5 sensor commercialised by the company Meter Environment (Pullman, USA). These sensors relate the average volumetric water content of the soil to the mean value of the dielectric constant over a volume of influence. The 10HS sensor covers a volume of influence of 1.3 dm^3 and detects volumetric water content in the range between 0 and 57%. The EC-5 sensor covers instead a smaller volume of influence of about 0.2 dm^3 but is characterised by a larger measurement range between 0 and 100% (the limit of 100% corresponds, of course, to the case where the sensor is immersed in water). Both sensors exhibit a measurement accuracy of ± 3% and can operate over a temperature range between 0 °C and 50 °C.

Measurements of both suction and volumetric water content were taken with hourly frequency over a period of at least three years with the only exception of station 203494 (Nouvelle Aquitaine, France), where field monitoring only lasted five months. This relatively long measurement period allowed validation of the proposed data quality assessment method under rather different seasonal climatic conditions.

4 ASSESSMENT OF REFERENCE WATER RETENTION CURVE PARAMETERS

The retention model parameters θ_r, θ_s, α and n were assessed by means of two alternative strategies. The first strategy relied on the direct measurement of the intrinsic soil properties consisting of clay fraction ($\%Clay$), sand fraction ($\%Sand$), dry density (ρ_d) and carbon content ($\%C$), which are then introduced in Equations (2), (3), (4) and (5). The second strategy consisted instead in a least square regression of field suction and volumetric water content data via Equation (1). This regression was performed by simultaneously optimising the values of $\%Clay$, $\%Sand$, ρ_d and $\%C$ inside Equations

(2), (3), (4) and (5), so that function given by Equation (1) provided the best match to the measured data. Both strategies are detailed in the following sections.

4.1 Direct measurement of intrinsic soil properties

The first approach is based on the direct measurement of intrinsic soil properties and was employed to select the parameters of the reference water retention curve at site 203494 (Nouvelle Aquitaine, France). The physical and mineralogical properties of the soil were determined in the laboratory according to standard experimental procedures. The grain size distribution was determined by dry sieving and sedimentation analysis in compliance with the norms AFNOR NFP94-056 (1996) and AFNOR NFP94-057 (1992), respectively. The dry density ρ_d was instead determined by assuming that the highest volumetric water content θ_{max} recorded by the station corresponded to a fully saturated soil state and therefore coincided with the porosity of the soil. The dry density ρ_d can then be calculated from the volumetric water content θ_{max} under saturated conditions by means of the following equation:

$$\rho_d = \frac{\rho_w \, G_s}{1 + G_s \theta_{max}} \tag{6}$$

where G_s is the specific gravity of soil grains and ρ_w is the density of the water equal to 1000 kg/m^3. The specific gravity G_s was determined by means of pycnometer tests according to the norm AFNOR NFP94-054 (1991) and was calculated as the average of three measurements. Finally, the soil organic matter was measured in compliance with the standard ASTM D2974 (2014) and the corresponding carbon content $\%C$ was calculated as 58% of the soil organic matter as suggested by Pribyl (2010).

The properties obtained from the above characterisation tests are summarised in Table 2, which shows that the soil is composed predominantly of sand with small fractions of silt and clay. The values in

Table 2 were then inserted in Equations (2), (3), (4) and (5) to determine the reference soil-water retention model parameters θ_r, θ_s, α and n, respectively.

4.2 Calibration via best-fitting of retention data

The second approach used to define the parameters of the reference water retention function is based on the best fit of Equations (1), (2), (3), (4) and (5) to field measurements of suction and volumetric water content and was employed to select the retention model parameters at the four sites 120A (Lower Austria, Austria), 235 (Alto Adige, Italy), 2287 (Puglia, Italy) and 1328 (Lower Austria, Austria).

A least square regression was performed by simultaneously varying the parameters $\%Clay$, $\%Sand$, $\%C$ and ρ_d in Equations (2), (3), (4) and (5) in order to achieve the best fit of Equation (1) to the field measurements of suction and volumetric water content. The silt fraction $\%Silt$ was subsequently calculated from the best fit values of $\%Clay$ and $\%Sand$ according to the following equation:

$$\%Silt = 100 - (\%Sand + \%Clay) \quad (7)$$

Figures 2(a), 2(b), 2(c) and 2(d) show the best fit curves obtained from the least square regression of Equation (1) to field data at sites 120A (Lower Austria, Austria), 235 (Alto Adige, Italy), 2287 (Puglia, Italy) and 1328 (Lower Austria, Austria), respectively. The corresponding values of the parameters $\%Sand$, $\%Silt$, $\%Clay$, ρ_d and $\%C$ are summarised in Table 3. Table 3 indicates a dominant sand fraction with a relatively small amount of clay at all sites with the only exception of site 235 (Alto Adige, Italy) where a dominant silt fraction was predicted.

5 VALIDATION OF THE REFERENCE WATER RETENTION CURVE

The reference water retention curve was validated by means of two alternative strategies. The first strategy consisted in comparing the reference water retention function against field measurements of suction and volumetric water content (not used for calibration for the case where the soil physical properties were determined by best-fitting of field data). The second strategy consisted in the comparison between field measurements of suction and volumetric water content at a given depth and the corresponding predictions of a Finite Element model of a soil column subjected to surface infiltration as monitored at the site. The former validation method was employed for sites 203494 (Nouvelle Aquitaine, France), 120A (Lower Austria, Austria), 235 (Alto Adige, Italy) and 2287 (Puglia, Italy) while the latter validation method was used for site 1328 (Lower Austria, Austria), as discussed in the following sections.

5.1 Validation via benchmarking against field water retention data

Figures 3 compare the reference soil-water retention curves with field data. All field data are plotted in Figure 3(a) for the case of site 203494 (Nouvelle Aquitaine, France), where water retention parameters were determined by direct measurement of soil physical properties. Only data not used for calibration are plotted for the case of sites 120A (Lower Austria, Austria), 235 (Alto Adige, Italy) and 2287 (Puglia, Italy), where the soil-water retention curve parameters were calibrated by best fitting an antecedent dataset of field measurements of suction and volumetric water content using.

Inspection of Figure 3 indicates that the field values of suction and volumetric water content are reasonably approximated by the reference water retention curve at all four sites. The relatively large scatter of field data might be caused by the effects of soil deformation and hydraulic hysteresis, which are not accounted for in the simple retention model adopted in this work.

Note that suction measurements at site 203494 (Nouvelle Aquitaine, France) were obtained by means of the Universal Tensiometer developed at the Université de Pau et des Pays de l'Adour in France (Mendes et al., 2016; Mendes et al., 2018), whose suction measuring range is relatively large up to 1500 kPa. Unfortunately, the measuring potential of this senor was not fully exploited because the measured suctions were limited to about 160 kPa due to the high precipitation rate recorded at the site during the monitoring period (Figure 3(a)).

Figure 3(b) shows two measurement anomalies at site 120A (Lower Austria, Austria), namely a decrease in suction at constant volumetric water content of about 0.09 and an increase of volumetric water content at constant suction of about 10 kPa. The former anomaly is due to a malfunctioning of the volumetric water content sensor while the latter one is due to the attainment of the low measurement limit of the suction sensor. Both these inconsistencies will be shown to detected by the proposed data quality assessment method as discussed later.

5.2 Validation via Finite Element simulations

The reference soil-water retention model was validated at site 1328 (Lower Austria, Austria) by comparing the results from the Finite Element simulation of water flow with the measured values of volumetric water content and suction. Site 1328 (Lower Austria, Austria) was chosen because of the absence of a hilly landscape around the monitoring station, which facilitated the treatment of water flow as a one-dimensional process. Figure 4 shows the geometry and boundary conditions of the one-dimensional Finite Element model together with the corresponding discretization mesh. The layer close to the surface was discretized with a finer mesh because most soil sensors were installed at shallow depths, thus particular attention was given to refining the upper part of the model.

The boundary condition at the top of the soil column consisted in the imposition of a net infiltration rate equal to the difference between the rainfall and evapotranspiration rates. The boundary conditions

at all other boundaries consisted in the imposition of a zero flux. The depth of the Finite Element model was fixed at 1.5m after performing a sensitivity analysis where the impervious boundary at the bottom was set at progressively increasing depths until no significant changes of model predictions were detected. At the initial time, the suction was set equal to the measured value at the ground surface with a hydrostatic variation underneath.

The rainfall rate was calculated from the daily precipitation measured at the site while the reference evapotranspiration rate ET_0 was estimated according to Monteith (1965) as:

$$ET_0 = \frac{\Delta(1-\alpha)R + \rho_a c_p e_s \frac{(1-RH)}{r_a}}{\Delta + \gamma(1+\frac{r_s}{r_a})} \quad (8)$$

where

- Δ is the slope of the saturated vapour pressure curve ($\delta e_o / \delta T$), where e_o = saturated vapour pressure (kPa) and T = daily mean temperature (°C)
- R is the (short wave) radiation flux
- α is the albedo assumed 0.23 as suggested by Allen et al. (1998)
- γ is the psychrometric constant (kPa °C^{-1}) given by $0.665 \cdot 10^{-3}$ P where P is the atmospheric pressure (kPa)
- ρ_a is the air density
- c_p is the specific heat of dry air, assumed $1.013 \cdot 10^{-3}$ (MJ kg^{-1} °C^{-1})
- e_s is the mean saturated vapour pressure
- r_a is the bulk surface aerodynamic resistance for water vapour
- RH is the ambient relative humidity
- r_s is the canopy surface resistance.

The aerodynamic resistance r_a was in turn calculated according to Allen et al. (1998) as:

$$r_a = \frac{ln\left[\frac{z_m - d}{z_{om}}\right] ln\left[\frac{z_h - d}{z_{oh}}\right]}{k^2 u_{zm}} \quad (9)$$

where

- z_m is the height of wind measurements (m)
- z_h is the height of humidity measurements (m)
- d is the distance from a reference plane (m) which can be estimated as $d = \frac{2}{3}h$ where h is the crop height assumed 0.12m.
- z_{om} is the roughness length governing momentum transfer (m) and assumed as *0.123h*
- z_{oh} is the roughness length governing transfer of heat and vapour (m) and assumed as $0.1z_{om}$
- k is the von Karman's constant, 0.41 (-)
- u_{zm} is the wind speed at height z_m (m s^{-1})

and the canopy resistance r_c was assumed equal to 50 s m^{-1} as suggested by Abtew et al. (1995).

The radiation flux *R*, the relative humidity *RH*, the temperature *T* and the wind speed u_{zm} were all measured at the site. The measurements were taken at 2m from the soil surface.

Figures 5 and 6 show the values of daily precipitation and evapotranspiration rates, which were used to define the net infiltration rate at the top of the soil column. The process of water flow was simulated over the period from June 2013 to December 2013, which is a sufficiently long interval of time to cover one cycle of wetting and drying. Any further extension in time would have augmented the computational burden without adding any value to the analysis.

By assuming that pore air pressure is always at the atmospheric value, the suction s coincides with the opposite of the pore water pressure and Darcy's law of permeability is therefore written as:

$$\vec{v} = -K\ grad(\Psi) = -Kgrad\left(z - \frac{s}{\gamma_w}\right) \quad (10)$$

where $\vec{v}$ is the water flux vector (i.e. the flow vector per unit area), Ψ is the piezometric head, K is the hydraulic conductivity, which depends on soil saturation, z is the vertical coordinate, which increases upwards and γ_w is the specific weight of the water. By further assuming that water is incompressible, the flow balance is written as:

$$\text{div}\ \vec{v} + \frac{\partial \theta}{\partial t} = 0 \tag{11}$$

where θ is the volumetric water content of the soil and t is the time. By substituting Equations (1) and (10) into Equation (11), Richard's equation is written in terms of soil suction s as:

$$C\frac{\partial s}{\partial t} = div[Kgrad\left(z - \frac{s}{\gamma_w}\right)] \tag{12}$$

where $C = \frac{\partial \theta}{\partial s}$ is the soil water capacity.

The water balance of Equation (12) was solved numerically via the Finite Element software SEEP/W, which is part of the commercial package Geostudio. Due to the lack of information regarding the variation of permeability with suction, a constant equivalent permeability $K = K_{eq}$ was adopted in the simulations. The adoption of a constant equivalent permeability is a strong approximation but the introduction of a dependency on suction would have added more uncertainties to the model with additional material parameters to be calibrated. Moreover, the use of a constant equivalent permeability improved significantly the convergence of the computer code. The value of equivalent permeability K_{eq} was estimated by best fitting the results from the finite element simulations to field measurements of suction and volumetric water content not used during validation.

Figure 7 compares the predicted and measured daily variations of volumetric water content (a) and suction (b) at a soil depth of 0.25 m for the weather station 1328. The equivalent permeability for this

site was estimated to be 10^{-9} m/s. Figure 7a indicates that the predicted volumetric water content is in good agreement with the measured value, which corroborates the validity of the chosen model for the reference water retention curve and its calibration against field data. Figure 7b shows instead that the predicted and measured values of suction match reasonably well only up to 400 kPa, which is the measuring limit of the suction sensor. Above this value, the measurement of suction levels off, as expected, while the prediction keeps increasing. The large fluctuation of predicted values as the soil becomes drier is due to the particular form of the soil-water retention curve, which predicts large variations of suction in correspondence of small variations of volumetric water content over the high suction range.

6 AUTOMATED DATA QUALITY ASSESSMENT CRITERION

This section describes the criterion employed to assess automatically the reliability of the field measurements of suction and volumetric water content. Two tolerance margins, $\Delta\theta$ and Δs, are introduced with respect to the measured values of volumetric water content and suction, θ_m and s_m, respectively, which define a "tolerance box" with sides equal to $2\Delta\theta$ and $2\Delta s$ centred around the measured data point (θ_m , s_m). If this tolerance box intersects the reference soil-water retention curve, the measured data point (θ_m , s_m) is accepted whereas a sensor malfunctioning is detected if the tolerance box does not intersect the reference soil-water retention curve (Figure 8).

The tolerance margins $\Delta\theta$ and Δs were defined as:

$$\Delta\theta = a_\theta + h_\theta \tag{13}$$

$$\Delta s = a_s + h_s \tag{14}$$

where a_θ and a_s are the accuracies of the volumetric water content and suction sensors, respectively, (see Section 3) while h_θ and h_s are the allowances of volumetric water content and suction, respectively, associated with the hysteretic behaviour of the soil. The tolerance margins of Equations

296 (13) and (14) have the purpose of avoiding an erroneous identification of faulty measurements. In
297 other words, these margins allow to discriminate between the physiological scatter of experimental
298 data (caused by both sensor accuracy and soil hysteresis) and the measurement deviation that is
299 instead produced by a malfunctioning of the sensor.

300 The water content allowance h_θ is here fixed to 1.5% while the suction allowance h_s varies from ±2.5
301 kPa, for suction values between 10 kPa and 50 kPa, to ±10% of the reading value, for suctions larger
302 than 50 kPa. This variation of the suction allowance h_s replicates the variation of the accuracy of the
303 MPS-1 sensor (see Section 3), which is mainly associated to the hysteretic retention behaviour of the
304 porous disk of the sensor. In other words, it is here assumed that the hysteretic responses of both the
305 MPS-1 sensor and the surrounding soil can be considered, in first instance, qualitatively similar. Note
306 that the definition of the tolerance margins given by Equations (13) and (14) is purely empirical but
307 a more theoretical (and perhaps more accurate) approach is possible, though this is outside the scope
308 of the present paper.

309 From the mathematical point of view, the tolerance criterion is described by the following four
310 inequalities, each of them with a precise geometrical meaning as discussed later:

$$[(\theta_m + \Delta\theta) - \theta\langle s_m - \Delta s\rangle] \cdot [(\theta_m - \Delta\theta) - \theta\langle s_m - \Delta s\rangle] \leq 0 \quad (15)$$

$$[(\theta_m + \Delta\theta) - \theta\langle s_m + \Delta s\rangle] \cdot [(\theta_m - \Delta\theta) - \theta\langle s_m + \Delta s\rangle] \leq 0 \quad (16)$$

$$[(s_m + \Delta s) - s\langle \theta_m - \Delta\theta\rangle] \cdot [(s_m - \Delta s) - s\langle \theta_m - \Delta\theta\rangle] \leq 0 \quad (17)$$

$$[(s_m + \Delta s) - s\langle \theta_m + \Delta\theta\rangle] \cdot [(s_m - \Delta s) - s\langle \theta_m + \Delta\theta\rangle] \leq 0 \quad (18)$$

311 In Equations (15) and (16), $\theta\langle s_m - \Delta s\rangle$ and $\theta\langle s_m + \Delta s\rangle$ are the values of the volumetric water content
312 calculated by the retention curve in correspondence of the two suction values $s_m - \Delta s$ and $s_m + \Delta s$,
313 respectively. Similarly, in Equations (17) and (18), $s\langle \theta_m - \Delta\theta\rangle$ and $s\langle \theta_m + \Delta\theta\rangle$ are the values of
314 suction calculated by the retention curve in correspondence of the two volumetric water content
315 values $\theta_m - \Delta\theta$ and $\theta_m + \Delta\theta$, respectively.

316 From the geometrical point of view, the verification of Equations (15), (16), (17) and (18) implies
317 that the water retention curve cuts through the left, right, bottom and top sides of the tolerance box,
318 respectively (Figure 8). Therefore, it suffices that at least one of the above inequalities is verified to
319 make sure that the retention curve touches the tolerance box and the data point is acceptable.
320 Conversely, if none of the above four inequalities is verified, the retention curve lies outside the
321 tolerance box and a sensor malfunctioning is detected. In this case, however, it is not possible to state
322 whether the malfunctioning concerns the volumetric water content or the suction sensor.

323 Note that the above considerations only apply to the most common case where the entire tolerance
324 box is located within the admissible volumetric water content range, which is delimited by the
325 saturated volumetric water content θ_s and the residual volumetric water content θ_r. From the
326 mathematical point of view, this corresponds to the case where the following inequality is satisfied
327 $\theta_s \geq \theta_m + \Delta\theta > \theta_m - \Delta\theta \geq \theta_r$.

328 If instead $\theta_m + \Delta\theta > \theta_s$, the retention curve cannot intercept the top side of the tolerance box, which
329 means that the left hand side of Equation (16) cannot be computed and this inequality must be
330 discarded. Similarly, if $\theta_r > \theta_m - \Delta\theta$, the retention curve cannot intercept the bottom side of the
331 tolerance box, which means that the left hand side of Equation (15) cannot be computed and this
332 inequality must be discarded. In both these cases, the number of available inequalities is therefore
333 reduced to three.

334 Finally, in the limit case where the entire tolerance lies outside the admissible volumetric water
335 content range, the retention curve cannot intercept any side of the tolerance box. This means that the
336 left hand sides of all four Equations (13), (14), (15) and (16) cannot be calculated and the data point
337 is automatically unacceptable. From the mathematical point of view this corresponds to the case
338 where one of the following two inequalities is satisfied $\theta_m + \Delta\theta > \theta_m - \Delta\theta > \theta_s$ or $\theta_r > \theta_m +$
339 $\Delta\theta > \theta_m - \Delta\theta$.

Figure 9 shows the application of the proposed criterion to the field measurements of suction and volumetric water content taken at the site 120A (Lower Austria, Austria). At this site, the volumetric water content was measured by means of a 10HS sensor with an accuracy of ±3%. The suction was instead measured by means of an MPS-1 with an accuracy of ±5 kPa over the range from 10 to 50 kPa and an accuracy of ±20%, for suctions larger than 50 kPa (see Section 3). These accuracies were introduced in Equations (11) and (12), together with the allowances of volumetric water content and suction associated to the hysteretic behaviour of the soil, to define the size of the tolerance box. Inspection of Figure 9 indicates that the proposed data assessment method was capable of detecting two different instances of confirmed sensor malfunctioning. In the first instance, the formation of ice on the volumetric water content sensor caused an interruption of the record, thus resulting in fictitious measurements of constant volumetric water content over a large range of suction. In the second case, the soil suction attained the lower limit of the sensor, which resulted in the erroneous measurement of variable volumetric water content at constant suction. This result indicates that the proposed data assessment method may allow the real time detection of sensor malfunctioning, thus enabling a timely intervention on the faulty station.

7 CONCLUSIONS

This paper has presented a method for the automated data quality assessment of field measurements of soil suction and volumetric water content to enable the real time detection of potential sensor malfunctioning. The method can therefore increase the reliability of in-situ measurements while providing a useful decision support tool for engineers, farmers and land managers.

The proposed method has been validated against data collected from five field stations installed by the company Pessl Instruments (Weiz, Austria) in five different agricultural soils in Austria, France and Italy. The proposed assessment method consists in defining a “tolerance box” centred around each field data point identified by a pair of suction and volumetric water content measurements. If

364 the tolerance box matches the predictions of the reference soil-water retention model, the suction and
365 volumetric water content sensors are assumed to work correctly. If instead the tolerance box does not
366 match the reference soil-water retention model, it is possible that at least one of the two sensors may
367 have failed. The size of the tolerance box is defined by considering the accuracies of the volumetric
368 water content and suction sensors plus the allowances associated to the hysteretic behaviour of the
369 soil. The application of the proposed data assessment method to the detection of two confirmed sensor
370 failures at one of the five monitored sites has proved the robustness of the approach.

371 The soil-water retention curve of Van Genuchten (1980) and the pedotransfer function of Vereecken
372 et al. (1989) have been chosen in this work due to the simplicity of the formulation and the possibility
373 of relating parameter values to intrinsic soil properties. This model presents however some
374 weaknesses such as the applicability only to a specific class of soils and the inability to reproduce
375 hydraulic hysteresis. The retention model was calibrated with data collected from the monitored sites
376 and was subsequently assessed against additional field data not used during calibration or against the
377 results of Finite Element simulations of groundwater infiltration at one of the monitored sites. The
378 validation showed that the chosen retention model can reproduce reasonably well the field behaviour
379 at all five sites. Of course, the same data assessment method can be combined with other models for
380 the reference soil-water retention provided that a consistent amount of field data is available to
381 calibrate and validate the chosen model.

382 ## ACKNOWLEDGEMENTS

383 The authors wish to thank the financial contribution of the European Commission to this research
384 through the Marie Curie Industry-Academia Partnership and Pathways Network MAGIC (Monitoring
385 systems to Assess Geotechnical Infrastructure subjected to Climatic hazards) – PIAPP-GA-2012-
386 324426.

387

8 REFERENCES

Abtew, W. 1996. Evapotranspiration measurements and modeling for three wet- land systems in South Florida. Journal of the American Water Resources Association, 127(3): 140–147.

AFNOR NFP94-054 (1991). Soils: investigation and testing – Determination of particle density-Pycnometer method.

AFNOR NFP94-057 (1992). Soils: investigation and testing – Granulometric analysis – Hydrometer method.

AFNOR NFP94-056 (1996). Soils: investigation and testing – Granulometric description – Dry sieving method.

Allen, R.G., Pereira, L.S., Raes, D., and Smith, M. 1998. Crop evapotranspiration: Guidelines for computing crop water requirements. FAO Irrigation and Drainage Paper 56.

ASTM D2974-14 (2014). Standard Test Methods for Moisture, Ash, and Organic Matter of Peat and Other Organic Soils, ASTM International, West Conshohocken, PA.

Brooks, R., & Corey, T. (1964). Hydraulic properties of porous media. *Hydrology Papers*, Colorado State University.

Fredlund, D. G., & Xing, A. (1994). Equations for the soil-water characteristic curve. *Canadian geotechnical journal*, 31(4), 521-532.

Gallipoli, D. (2012). A hysteretic soil-water retention model accounting for cyclic variations of suction and void ratio. *Geotechnique*, 62(7), 605.

Gallipoli, D., Bruno, A. W., D'Onza, F., & Mancuso, C. (2015). A bounding surface hysteretic water retention model for deformable soils. *Géotechnique*, 65(10), 793-804.

Gallipoli, D., Wheeler, S. J., & Karstunen, M. (2003). Modelling the variation of degree of saturation in a deformable unsaturated soil. *Géotechnique*, 53(1), 105-112.

Khalili, N., Habte, M. A., & Zargarbashi, S. (2008). A fully coupled flow deformation model for cyclic analysis of unsaturated soils including hydraulic and mechanical hystereses. *Computers and Geotechnics*, 35(6), 872-889.

Mašín, D. (2010). Predicting the dependency of a degree of saturation on void ratio and suction using effective stress principle for unsaturated soils. *International Journal for Numerical and* Analytical Methods in Geomechanics, 34(1), 73-90.

Mendes, J., Gallipoli, D., Boeck,F., von Unold , G., & Tarantino, A. (2016). Building the UPPA high capacity tensiometer. In Proceedings 3rd European Conference on Unsaturated Soils. Paris, France, 12-14 September 2016.

Mendes, J., Gallipoli, D., Toll, D.G., & Tarantino, A. (2018). First saturation and resaturation of High Capacity Tensiometers with 1.5MPa High Air Entry Value (HAEV) ceramic filters. In Proceedings 2nd Pan American Conference on Unsaturated Soils: 514-522. Dallas, USA, 12-15 November 2017, ASCE Geotechnical Special Publication No. 301.

Mendes, J., Toll, D.G., Augarde, C.E., & Gallipoli, D. (2008). A system for field measurement of suction using high capacity tensiometers. In Proceedings 1st European Conference on Unsaturated Soils: 219-225. Durham, United Kingdom, 2-4 July 2008, CRC Press, ISBN: 9780203884430.

Molchanov, E. N. (2011). Soil monitoring: Methodology and realization. *Eurasian Soil Science*, *44*(2), 245–246.

Monteith, J.L. (1965) Evaporation and the Environment. *19th Symposia of the Society for Experimental Biology*, 19, 205-234

Nuth, M., & Laloui, L. (2008). Advances in modelling hysteretic water retention curve in deformable soils. *Computers and Geotechnics*, 35(6), 835-844.

Pooja, S., Uday, D. V., Nagesh, U. B., & Talekar, S. G. (2017, December). Application of MQTT protocol for real time weather monitoring and precision farming. In *2017 International Conference on Electrical, Electronics, Communication, Computer, and Optimization Techniques (ICEECCOT)* (pp. 1-6). IEEE.

Pribyl, D. W. (2010). A critical review of the conventional SOC to SOM conversion factor. *Geoderma*, 156(3), 75-83.

Salager, S., El Youssoufi, M. S., & Saix, C. (2010). Definition and experimental determination of a soil-water retention surface. *Canadian Geotechnical Journal*, 47(6), 609-622.

Stenberg, B. (1999). Monitoring Soil Quality of Arable Land: Microbiological Indicators. *Acta Agriculturae Scandinavica Section B: Soil and Plant Science*, *49*(1), 1–24. https://doi.org/10.1080/09064719950135669

Sun, D. A., Sheng, D., Xiang, L., & Sloan, S. W. (2008). Elastoplastic prediction of hydro-mechanical behaviour of unsaturated soils under undrained conditions. *Computers and Geotechnics*, 35(6), 845-852.

Supit, I., Van Diepen, C. A., De Wit, A. J. W., Wolf, J., Kabat, P., Baruth, B., & Ludwig, F. (2012). Assessing climate change effects on European crop yields using the Crop Growth Monitoring System and a weather generator. *Agricultural and Forest Meteorology*, 164, 96-111.

Tarantino, A. (2009). A water retention model for deformable soils. *Géotechnique*, 59(9), 751-762.

Van Genuchten, M. T. (1980). A closed-form equation for predicting the hydraulic conductivity of unsaturated soils. *Soil science society of America journal*, 44(5), 892-898.

Vereecken, H., Maes, J., Feyen, J., & Darius, P. (1989). Estimating the soil moisture retention characteristic from texture, bulk density, and carbon content. *Soil science*, 148(6), 389-403.

Vicente-Guijalba, F., Martinez-Marin, T., & Lopez-Sanchez, J. M. (2014). Dynamical approach for real-time monitoring of agricultural crops. *IEEE Transactions on Geoscience and Remote Sensing*, 53(6), 3278-3293.

Wheeler, S. J., Sharma, R. S., & Buisson, M. S. R. (2003). Coupling of hydraulic hysteresis and stress–strain behaviour in unsaturated soils. *Géotechnique*, 53(1), 41-54.

Zhou, A. N., Sheng, D., Sloan, S. W., & Gens, A. (2012). Interpretation of unsaturated soil behaviour in the stress–Saturation space, I: Volume change and water retention behaviour. *Computers and Geotechnics*, 43, 178-187.

TABLES

Table 1. Field stations: installation site and soil sensors

Field station	Site	Latitude	Longitude	Number and type of soil sensors	Depth
1328	Lower Austria, Austria	48.4839° N	15.6410° E	N° 2 - 10HS Soil Moisture (volumetric water content)	10 and 25 cm
				N° 1 - MPS-1 (suction)	10 cm
120A	Lower Austria, Austria	47.9005° N	16.9221° E	N° 2 - 10HS Soil Moisture (volumetric water content)	10 and 25 cm
				N° 1 - MPS-1 (suction)	10 cm
				N° 3 - MPS-6 (suction)	25 cm
203494	Nouvelle Aquitaine, France	43.5456° N	1.0972° W	N° 2 – EC5 Soil Moisture (volumetric water content)	10 and 25 cm
				N° 1 - MPS-6 (suction)	10 cm
				N° 1 - Universal Tensiometer (suction)	25 cm
235	Alto Adige, Italy	46.3089° N	11.2773° E	N° 2 - 10HS Soil Moisture (volumetric water content)	10 and 25 cm
				N° 1 - MPS-1 (suction)	10 cm
2287	Puglia, Italy	40.3601° N	17.4100° E	N° 2 - 10HS Soil Moisture (volumetric water content)	10 and 25 cm
				N° 2 – MPS-6 (suction)	10 and 25 cm

Table 2. Measured soil properties: field station 203494

G_s	ρ_d	$\%C$	Grain Size Distribution		
			$\%Sand$	$\%Silt$	$\%Clay$
			[0.063 – 2 mm]	[0.002 – 0.036 mm]	[<0.002 mm]
-	*g/cm³*	*%*	*%*	*%*	*%*
2.59	1.45	1.19	92.5	6.7	0.8

Table 3. Calibrated soil properties: field stations 120A, 235, 2287 and 1328

Field station	$\%Sand$ *%*	$\%Silt$ *%*	$\%Clay$ *%*	ρ_d *g/cm³*	$\%C$ *%*
120A	100.0	0.0	0.0	2.22	4.5
235	25.8	52.1	22.1	2	0.1
2287	81.1	0.9	18.0	2.05	0.25
1328	65.1	20	14.9	1.95	0.2

FIGURES

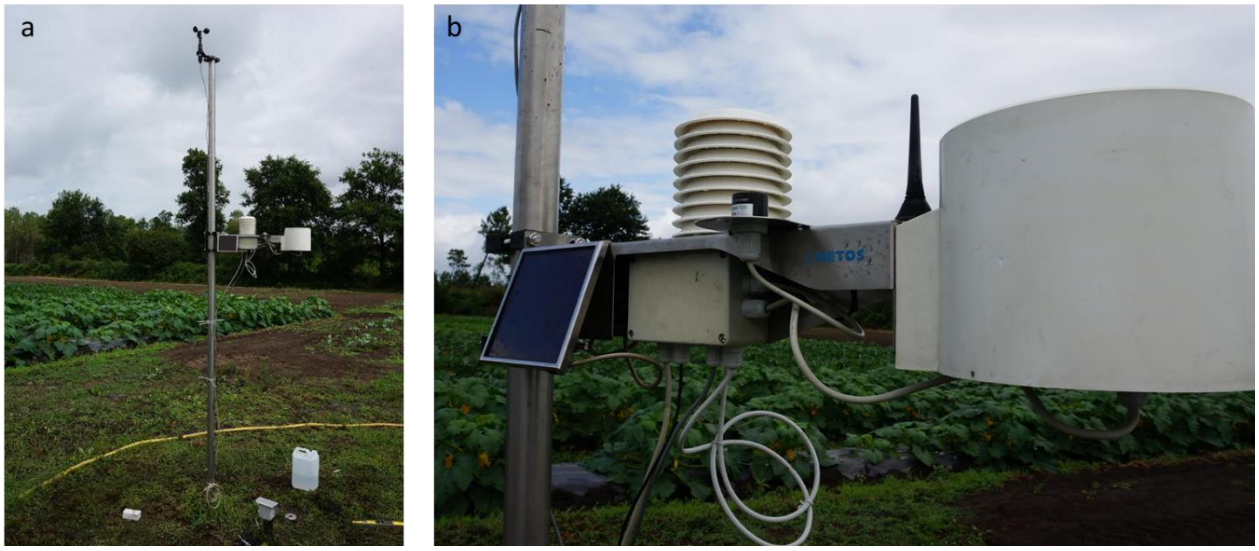

Figure 1. Typical field station installation (a) and detail of sensor connections to internet data logger (b)

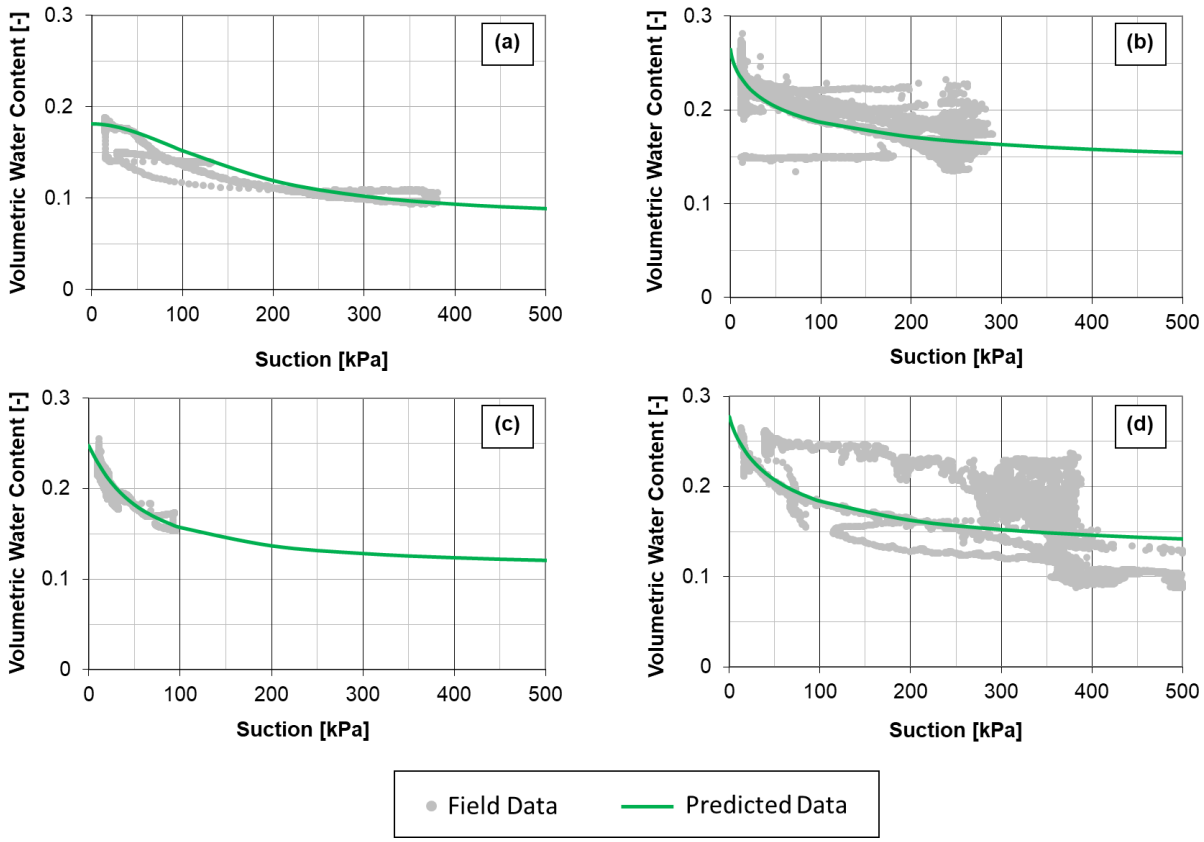

Figure 2. Calibration of intrinsic soil properties used to characterise the reference water retention curve: field stations 120A (a), 235 (b), 2287 (c) and 1328 (d)

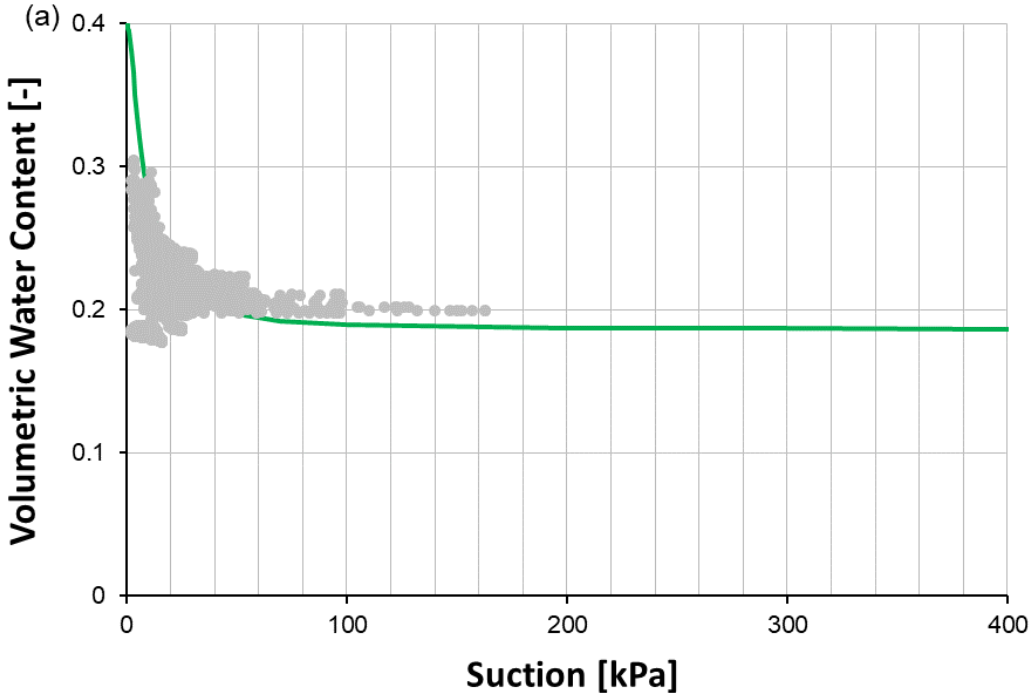
(a)
Volumetric Water Content [-]
0.4
0.3
0.2
0.1
0
0
100
200
300
400
Suction [kPa]

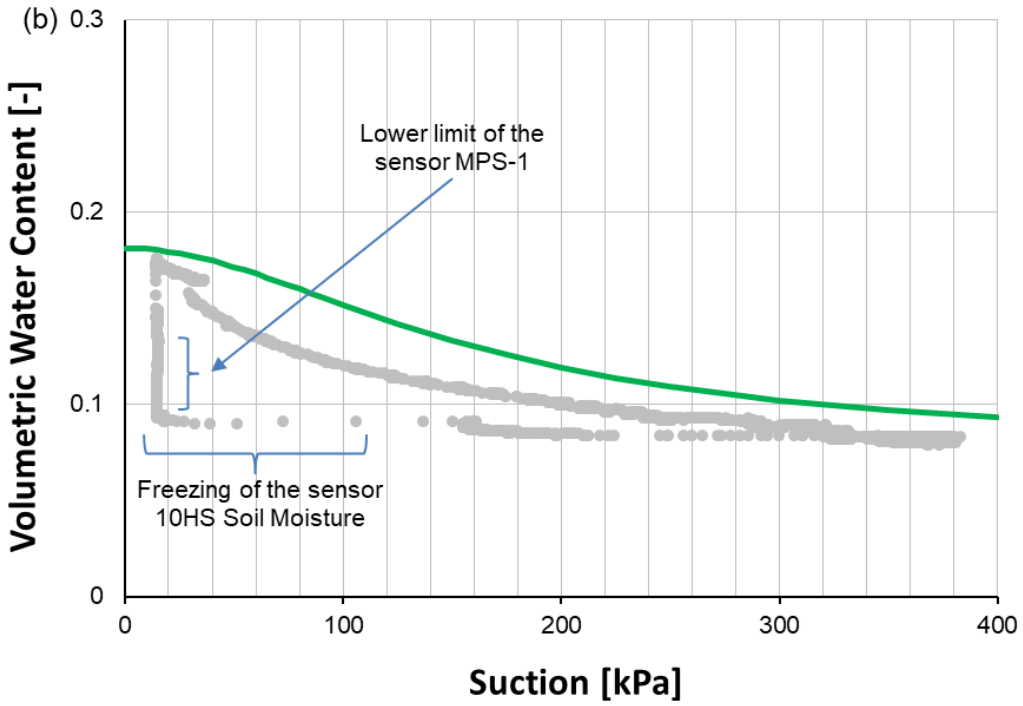
(b)
Volumetric Water Content [-]
0.3
0.2
0.1
0
Lower limit of the sensor MPS-1
Freezing of the sensor 10HS Soil Moisture
0
100
200
300
400
Suction [kPa]

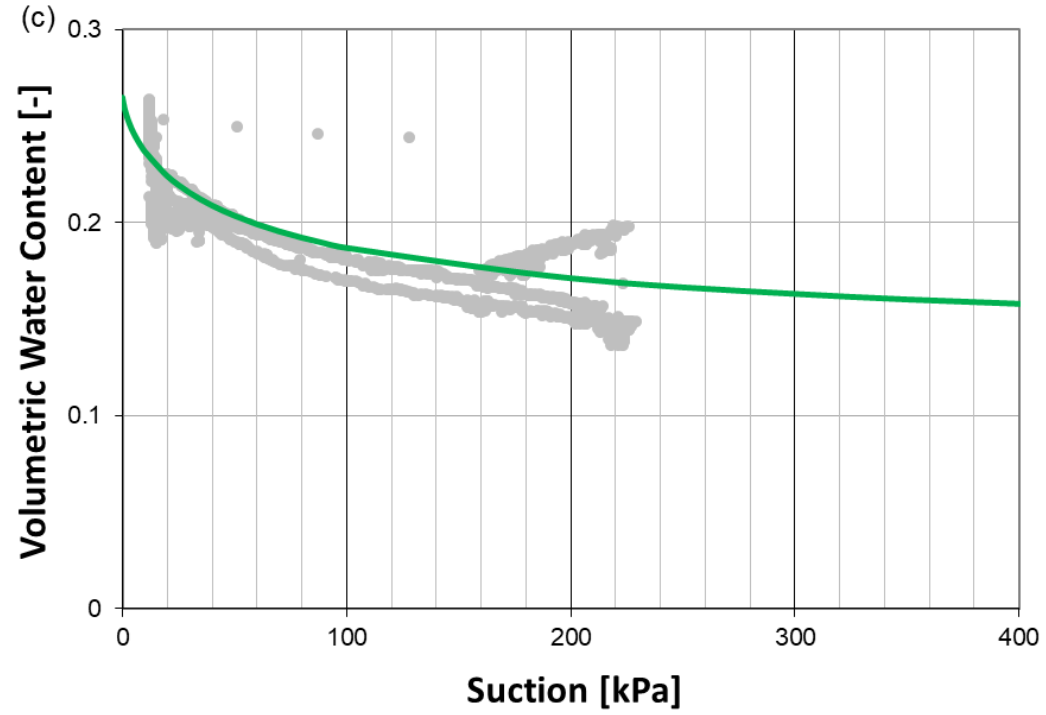

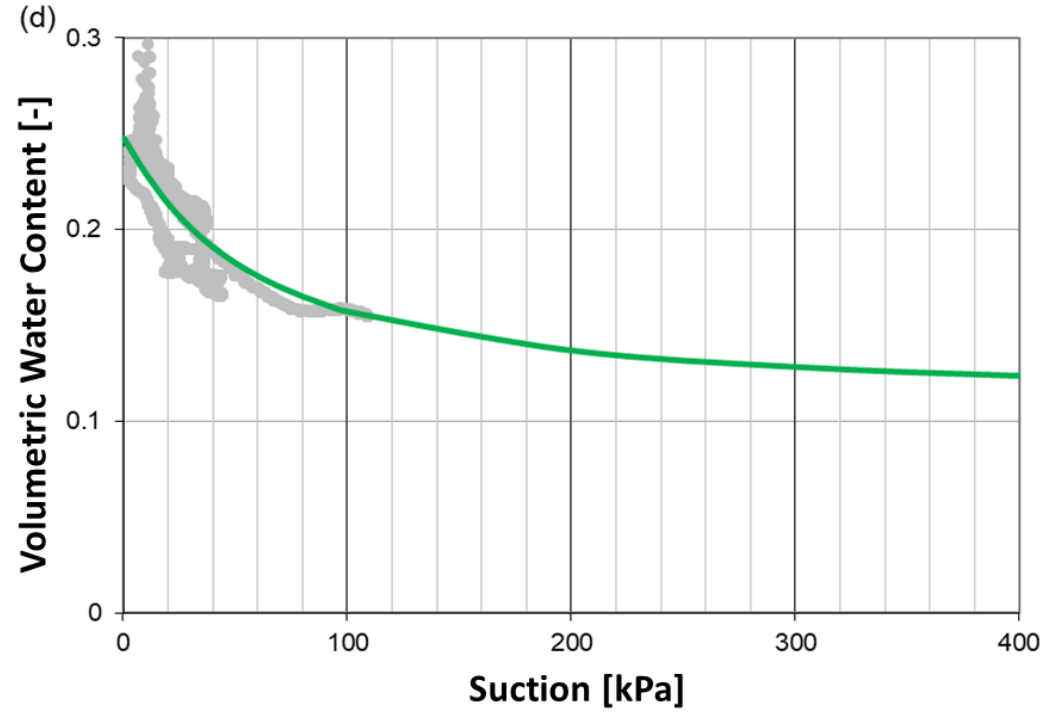

Figure 3. Validation of the calibrated reference water retention curve against water retention measurements not used for calibration: field stations 203494 (a), 120A (b), 235 (c) and 2287 (d)

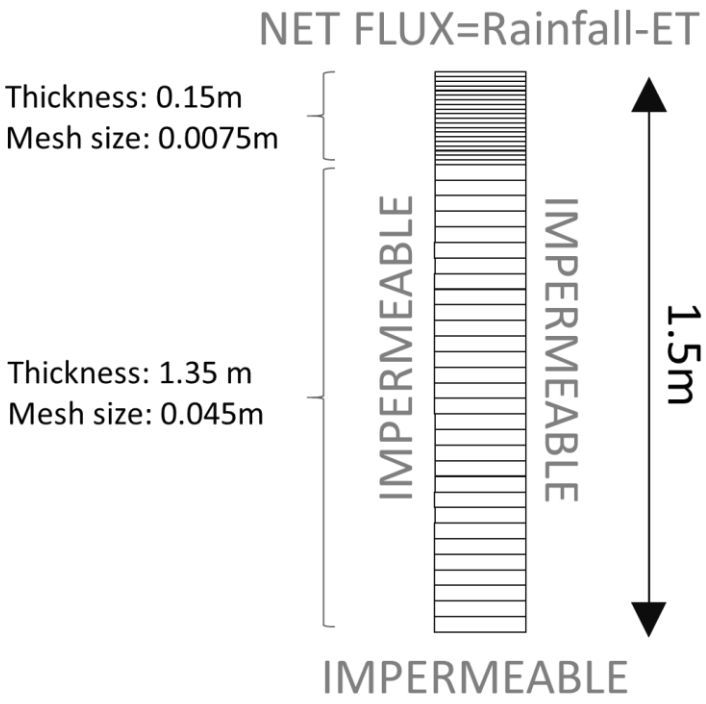

Figure 4. Geometry and boundary conditions of one-dimensional Finite Element mesh

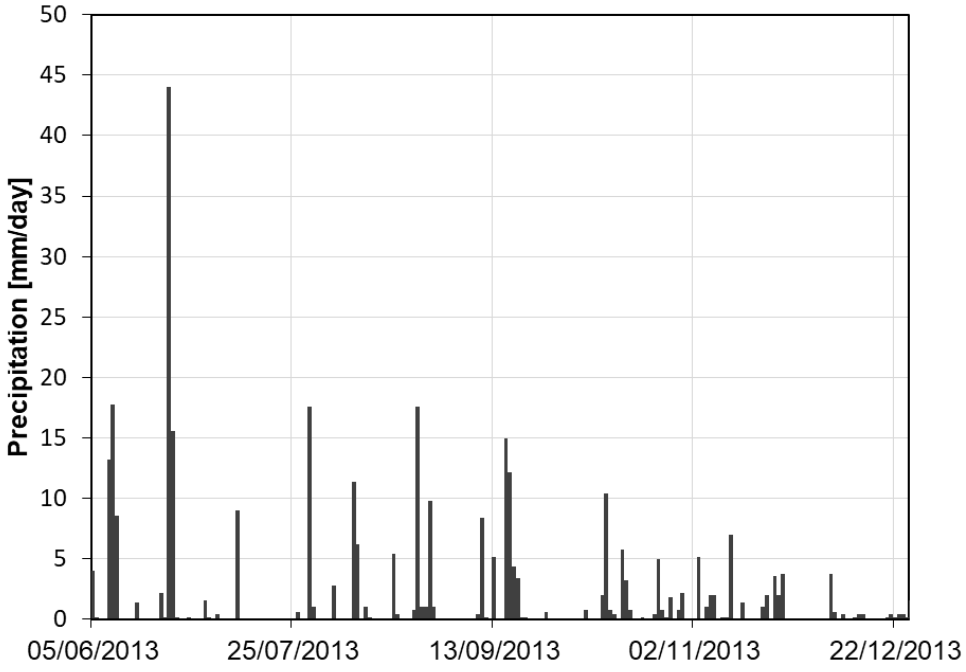

Figure 5. Daily precipitation recorded by field station 1328

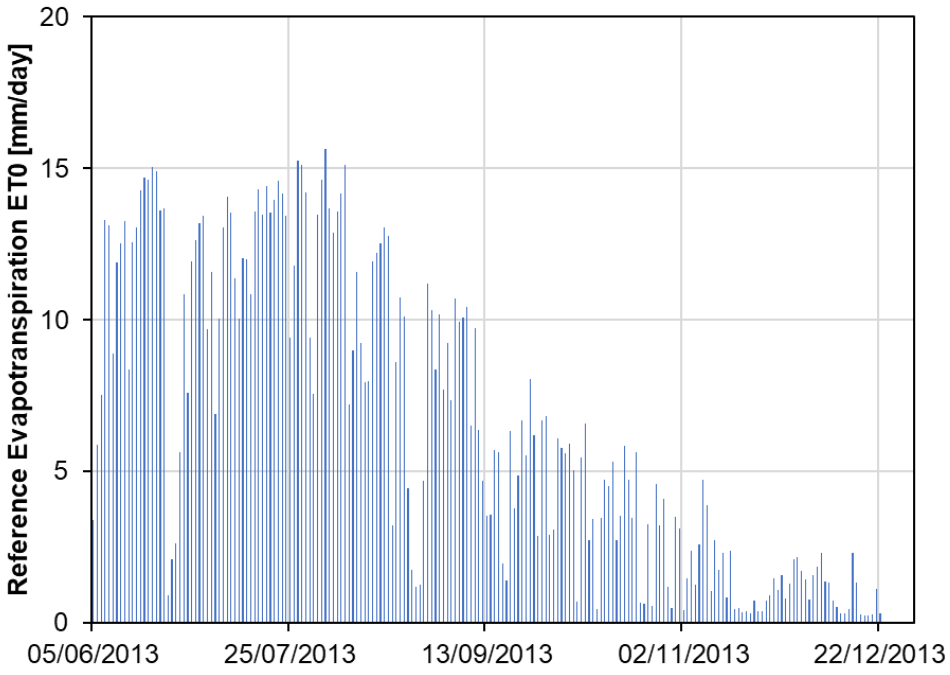

Figure 6. Reference Daily evapotranspiration calculated according to Monteith (1965)

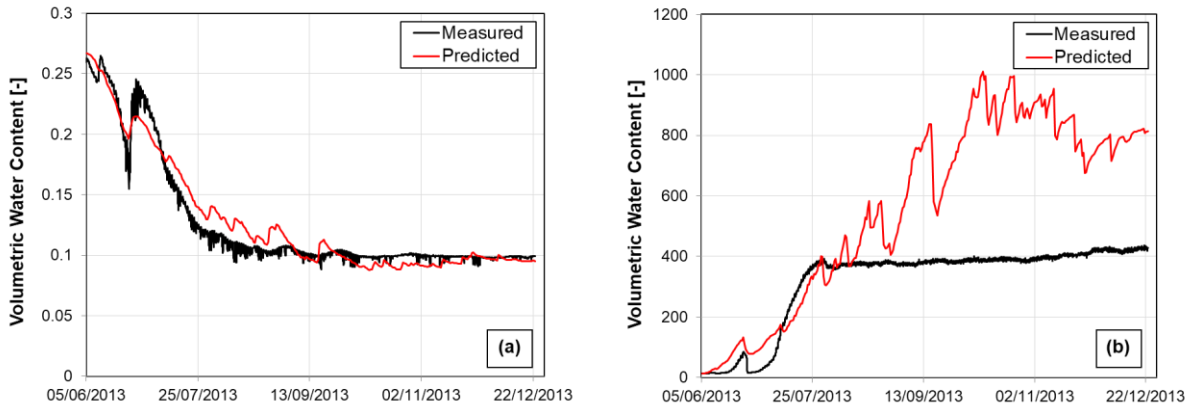

Figure 7. Water retention function validation by comparison of calculated and measured values of water content (a) and suction (b) at a depth of 0.25m: field station 1328

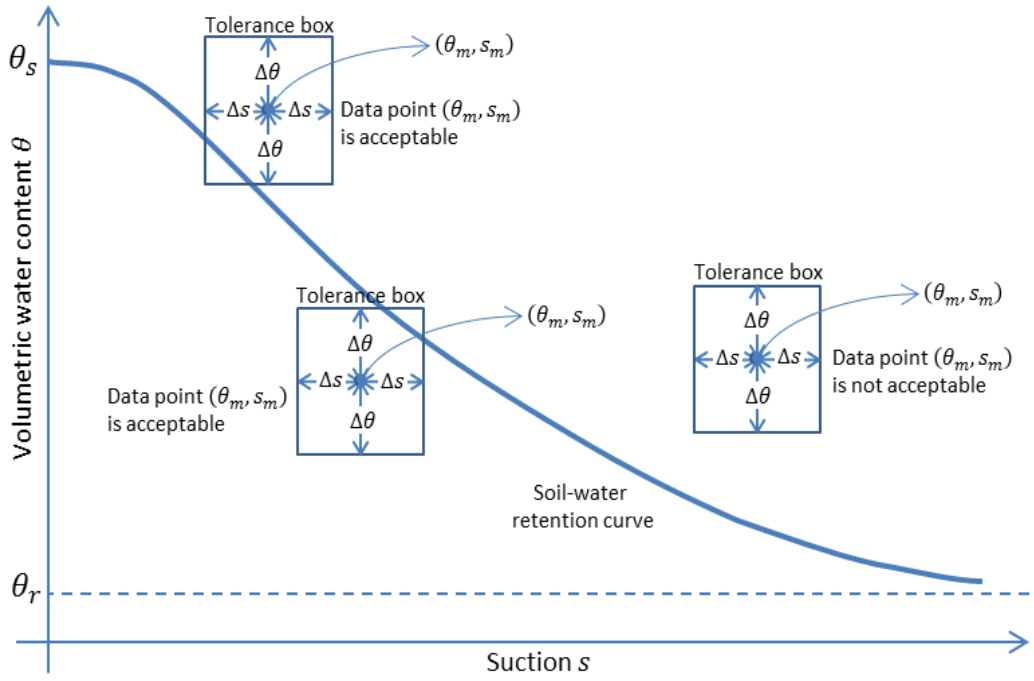

Figure 8. Schematic representation of proposed data assessment method

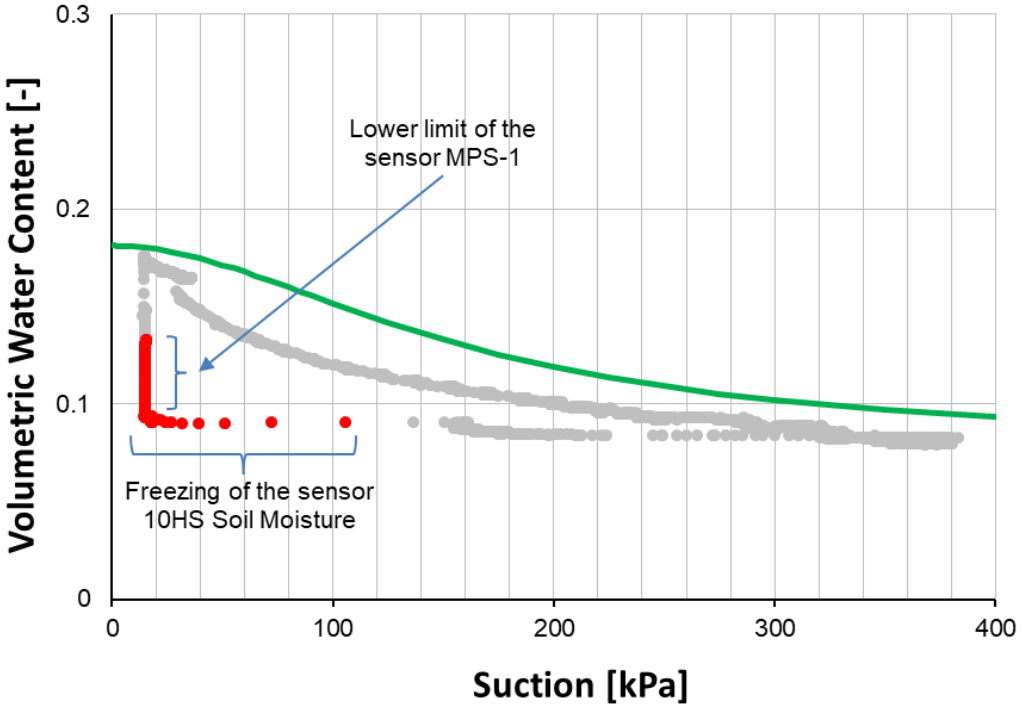

Figure 9. Application of proposed data assessment method to station 120A